Electronic Supplementary Information (ESI)

Efficient homogeneous electrocatalytic hydrogen evolution using a Ni-containing polyoxometalate catalyst

Debu Jana, Hema Kumari Kolli, Subhashree Sabnam and Samar K. Das*

School of Chemistry, University of Hyderabad, P.O. Central University, Hyderabad – 500046, India

Table of Contents:

Section S1. Physical measurements:

The compound **1** was synthesized and characterized by single crystal XRD, Powder X-ray diffraction, FT-IR, Raman, UV-Visible, Thermogravimetric analysis, FESEM imaging techniques and electrochemistry.

Single crystal X-ray data of **1** was collected from Bruker D8 Quest diffractometer fitted with a Photon 100 CMOS area detector system under Mo-K_α (λ = 0.71073 Å) graphite monochromated X-ray beam. FT-IR spectra of **1** was recorded by an iD7 ATR thermo Fisher Scientific-Nicolet iS5 instrument. Thermogravimetric (TGA) analyses were carried out on a STA 409 PC analyzer. Field emission Scanning Electron Microscope (FESEM) imaging and energy dispersive X-ray (EDX) spectroscopy were carried out on a Carl Zeiss model Ultra 55 microscope: EDX spectra and maps were recorded using Oxford instruments X-MaxN SDD (50 mm2) system and INCA analysis software. All electrochemical experiments were performed using a Zahner Zanium electrochemical work station operated with Thales software.

Section S2. Experimental section:

Synthesis of compound 1: A 55mL solution of $NaVO_3$ (2.6g, 21.32mmol) was heated at 70°C for 1 hour to get a clear solution. The solution was allowed to cool to room temperature, subsequently 50mL of acetic acid (99.5%) was added to maintain the pH value of 2.8, followed by addition of 10mL of $NiCl_2.6H_2O$ (1.27g, 5.34mmol) with constant stirring. Then 10mL solution of KCl (1g, 13.41mmol) was mixed slowly to it and stirring was stopped immediately to avoid formation of precipitates. Then the mixture was kept undisturbed for crystallization. After 48 hours, small yellow-colored crystals were obtained and collected by filtration and finally dried in air. Yield: 83% (based on V), $H_{32}K_2Ni_2O_{44}V_{10}$ (Molecular weight 1441.2).

Synthesis of $Na_6V_{10}O_{28}.18H_2O$[1]: A 100mL solution of $NaVO_3$ (3g, 24.6mmol) was prepared by heating the solution for 2 hours at 70°C. The solution was allowed to cool to room temperature, subsequently 4M HCl was added to maintain a pH of 4.5. Further to the solution, 200mL of ethanol (96%) was added to get orange crystals. The solid obtained was filtered and dried in air. Yield: 54% (based on V), $Na_6H_{36}V_{10}O_{46}$ (Molecular weight 1419.6).

Section S3. Single crystal XRD data of compound 1:

Table S1: Selected List of Bond lengths and Bond angles of compound **1**

Bond angles		Bond lengths	
O(18)-Ni(1)-K(1)	58.15(14)	Ni(1)-O(18)	2.035(4)
O(17)-Ni(1)-K(1)	118.19(13)	Ni(1)-O(17)	2.064(4)
O(20)-Ni(1)-K(1)	131.90(13)	Ni(1)-O(20)	2.052(4)
O(16)-Ni(1)-K(1)	126.53(13)	Ni(1)-O(16)	2.042(4)
O(15)-Ni(1)-K(1)	48.83(13)	Ni(1)-O(15)	2.054(4)
O(19)-Ni(1)-K(1)	50.93(12)	Ni(1)-O(19)	2.071(4)
V(3)-O(10)-K(1)#2	101.35(15)	Ni(1)-K(1)	3.8288(17)
V(4)-O(10)-K(1)#2	140.8(2)	V(5)-V(3)#1	3.0670(12)
Ni(1)-O(15)-K(1)	99.20(16)	V(5)-V(1)	3.0842(12)
V(4)-O(11)-K(1)#3	133.3(2)	V(2)-V(4)#1	3.0542(12)
Ni(1)-O(19)-K(1)	96.57(14)	V(4)-V(3)	3.0915(13)
V(2)-O(6)-K(1)#4	136.9(2)	V(1)-V(3)	3.0776(13)
Ni(1)-O(18)-K(1)	89.74(15)	V(3)-K(1)#2	3.6216(16)
V(1)-O(1)-K(1)	138.0(2)		
V(3)-O(9)-K(1)#2	99.76(18)		
O(6)#4-K(1)-V(3)#2	168.61(10)		
O(22)#5-K(1)-V(3)#2	97.87(11)		
O(10)#2-K(1)-V(3)#2	29.83(8)		
O(15)-K(1)-V(3)#2	104.94(9)		
O(9)#2-K(1)-V(3)#2	25.91(7)		
O(19)-K(1)-V(3)#2	72.46(8)		
O(1)-K(1)-V(3)#2	91.08(9)		
O(21)#5-K(1)-V(3)#2	68.05(10)		
O(18)-K(1)-V(3)#2	124.91(8)		
O(6)#4-K(1)-Ni(1)	90.38(9)		
O(22)#5-K(1)-Ni(1)	148.36(11)		
O(10)#2-K(1)-Ni(1)	82.50(9)		
O(15)-K(1)-Ni(1)	31.98(8)		
O(9)#2-K(1)-Ni(1)	120.49(9)		
O(19)-K(1)-Ni(1)	32.51(8)		
O(1)-K(1)-Ni(1)	89.12(9)		
O(21)#5-K(1)-Ni(1)	143.34(10)		
O(18)-K(1)-Ni(1)	32.11(7)		
V(3)#2-K(1)-Ni(1)	101.00(4)		

Symmetry transformations used to generate equivalent atoms:

#1 -x+1,-y+1,-z+1 #2 -x+1,-y,-z+2 #3 x,y,z-1

#4 -x+1,-y+1,-z+2 #5 -x+2,-y,-z+2 #6 x,y,z+1

Table S2: Crystal data and structure refinement parameters for compound **1**

Empirical formula	$H_{32}K_2Ni_2O_{44}V_{10}$	
Formula weight	1441.27	
Temperature	293(2) K	
Wavelength	0.71073 Å	
Crystal system	Triclinic	
Space group	P -1	
Unit cell dimensions	a = 8.7397(4) Å	α = 65.037(4)°
	b = 10.7629(5) Å	β = 75.059(4)°
	c = 11.1283(5) Å	γ = 70.540(4)°
Volume	886.32(8) $Å^3$	
Z	1	
Density (calculated)	2.700 mg/m^3	
Absorption coefficient	3.914 mm^{-1}	
F(000)	708	
Goodness-of-fit on F^2	1.042	
Final R indices [I>2σ (I)]	R1 = 0.0725, wR2 = 0.1967	
R indices (all data)	R1 = 0.0771, wR2 = 0.2074	
Largest diff. peak and hole	1.495 and -1.570 $e.Å^{-3}$	

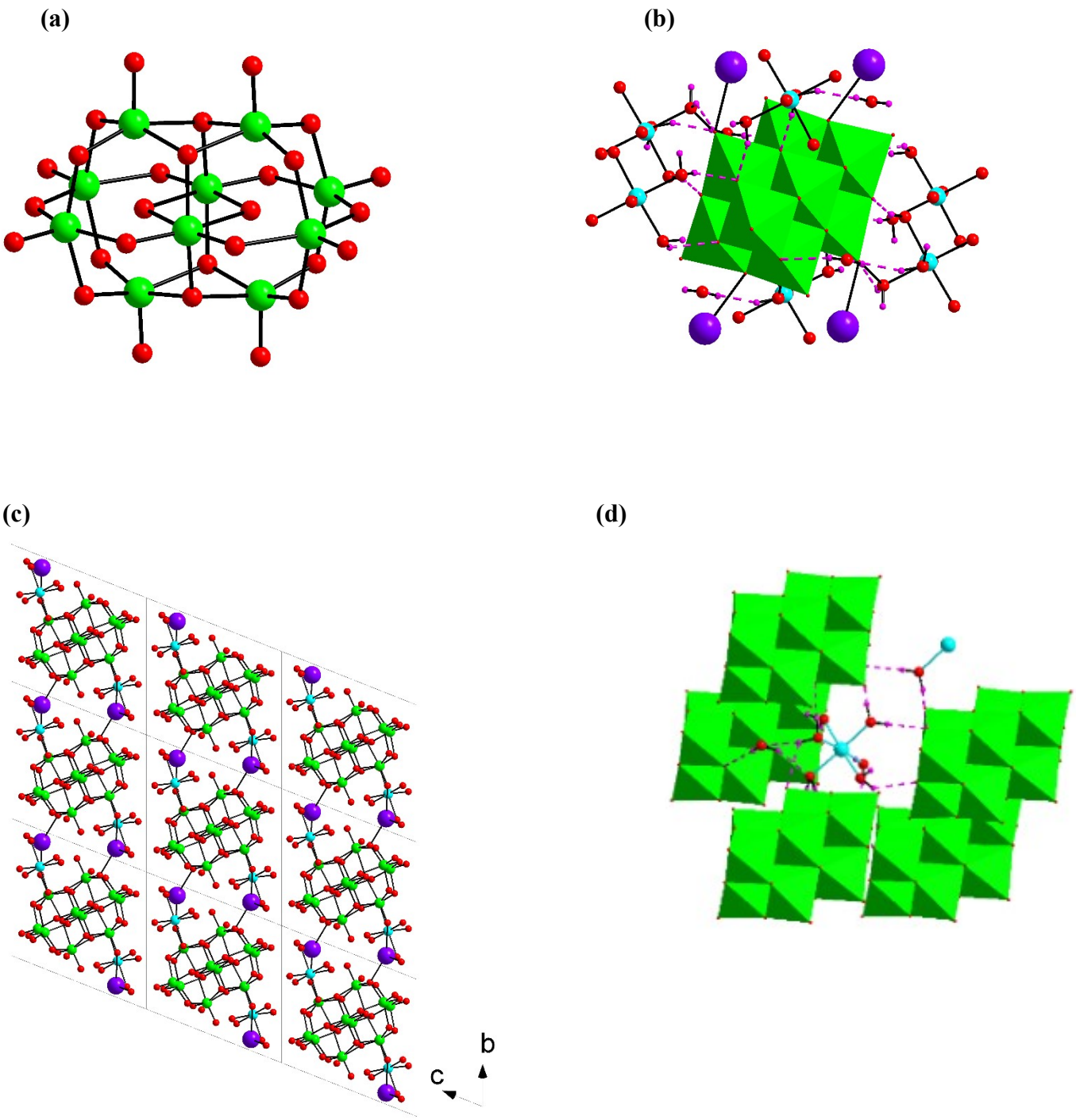

Fig. S1. (a) Structural drawing of decavanadate anion $[V_{10}O_{28}]^{6-}$ found in the crystal structure of compound $K_2[Ni(H_2O)_6]_2[V_{10}O_{28}]\cdot 4H_2O$ (**1**); (b) Coordination and hydrogen bonding environment around the decavanadate cluster (polyhedral representation) anion and (c) 3×3×3 supercell in the crystal structure of compound **1**; (d) Hydrogen bonding (O−H···O) situation around $\{Ni(H_2O)_6\}^{2+}$, where all six nickel-coordinated water molecules are exclusively hydrogen bonded to decavanadate cluster oxygens. Color code: V, green; K, purple; Ni, cyan; O, red; H, pink; hydrogen bonds are shown by dotted lines.

Section S4. FT-IR analysis of compound 1:

Compound **1** is characterized by Infrared spectrum performed on JASCO-5300 FT-IR spectrophotometer. The IR bands appeared in the 955 - 811 cm^{-1} region (**Figure S2**) due to the V=O stretching vibrations and bands in the 750 – 600 cm^{-1} due to vibration of bridging V-O-V groups. The IR stretching in the region of 3151 cm^{-1} is due to the O-H stretching. The band at 1616 cm^{-1} is due to the H-O-H bending.

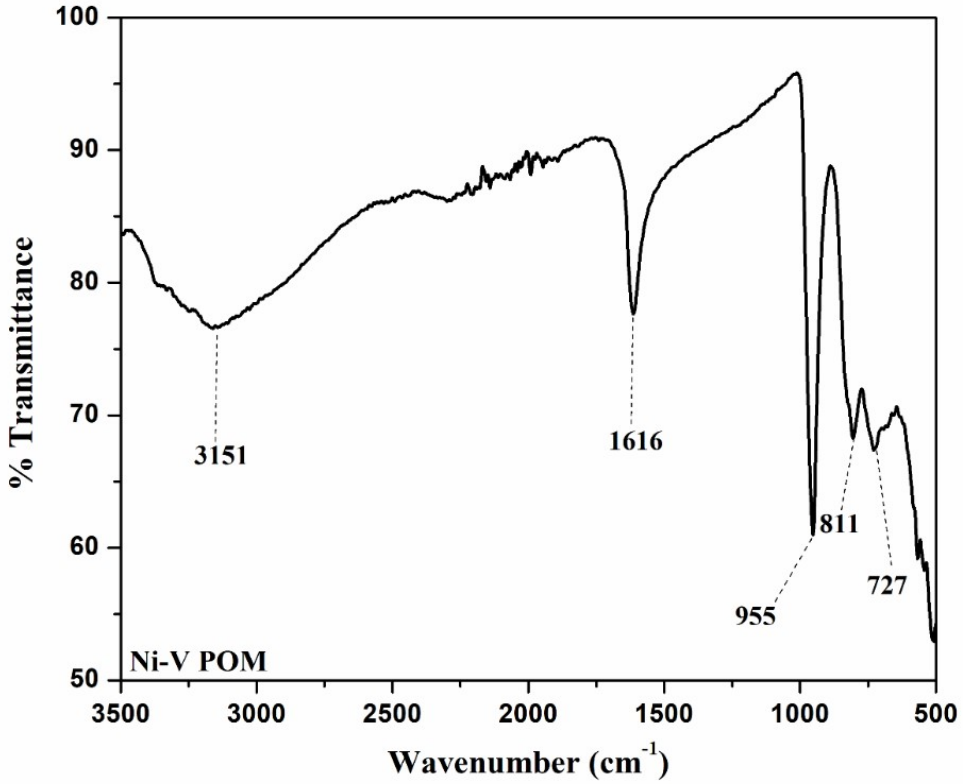

Fig. S2. FT-IR spectrum of compound **1**.

Section S5. PXRD analysis of compound 1:

PXRD pattern of synthesized compound **1,** completely matches with the simulated pattern.

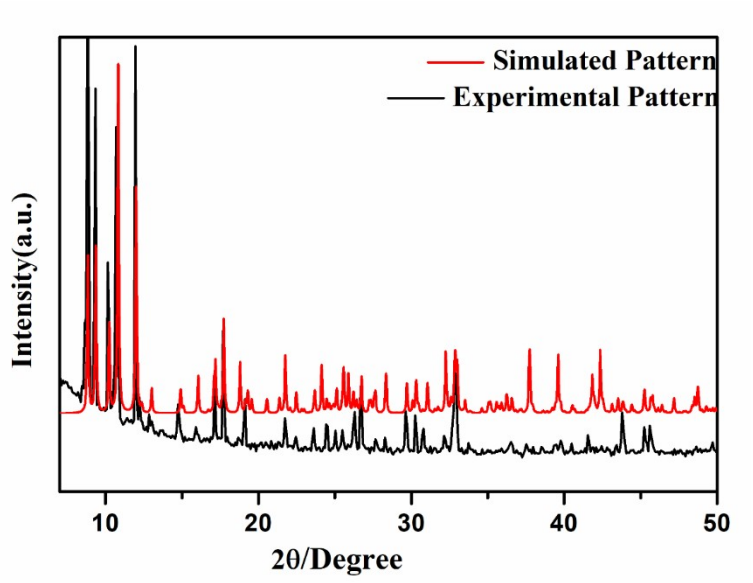

Fig. S3. PXRD patterns of compound **1**.

Section S6. Raman spectral analysis of compound 1:

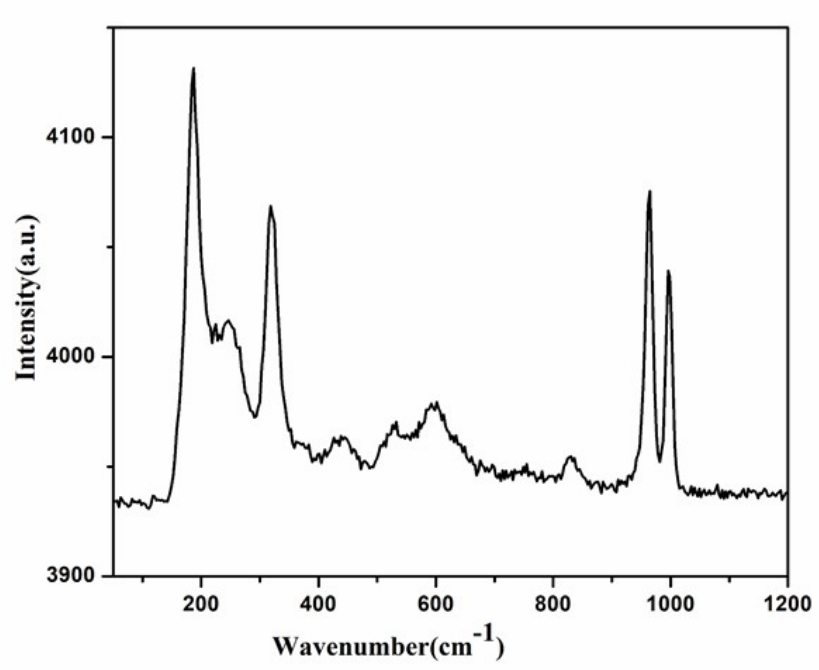

Fig. S4. Raman spectrum of compound **1**.

Raman Spectra of compound **1** has been recorded at the wavelength 632 nm. In the Raman spectrum, bands appeared in 996 –957 cm^{-1} region is due to the V=O group. The Raman band appeared around 830 cm^{-1} (**Figure S4**) due to the V-O-V vibration.

Section S7. Thermogravimetric analysis of compound 1:

Thermogravimetric analysis (TGA) of compound **1** has been performed in N_2 atmosphere in the temperature range of 30 – 800 ^oC. The compound **1** undergoes weight loss. In case of compound **1**, the weight loss at 250^0C due to loss of water molecules (**Figure S5**).

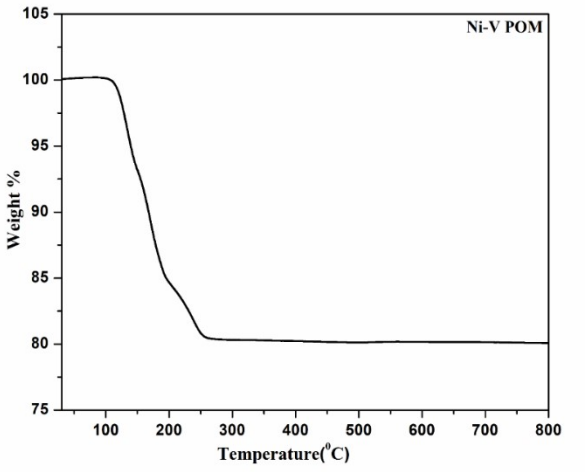

Fig. S5. TGA plot of compound **1**.

Section S8. Solid state UV-visible spectroscopy of compound 1

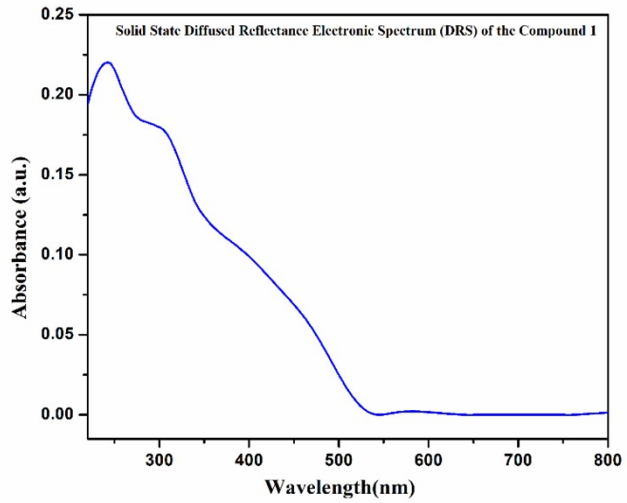

Fig. S6. Kubelka-Munk converted solid state diffused reflectance spectrum (DRS) of the compound **1**.

Section S9. Field Emission Scanning Electron Microscopy (FESEM) and Energy-dispersive X-ray (EDX) analysis of compound 1

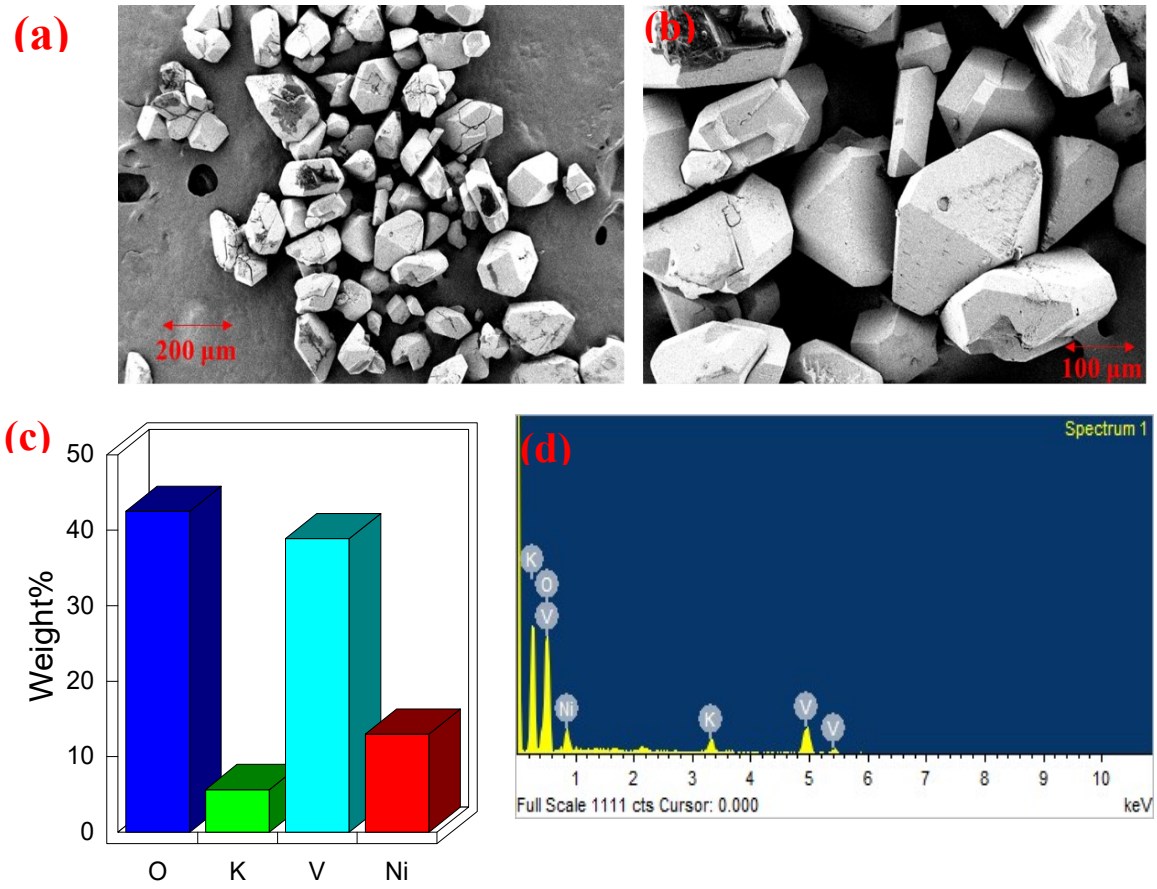

Fig. S7. (a) and (b) FESEM images of compound **1**, (c) and (d) EDX histograms of compound **1**.

Section S10. Electrochemical study and analysis:

All the electrochemical measurements were performed in homogeneous medium using three-electrode electrochemical cell where glassy carbon (GC) electrode and carbon paper electrode as working electrode, Ag/AgCl (3M KCl) electrode as reference electrode and Pt wire as counter electrode were used. The sample was prepared by dissolving 7.2 mg of compound **1** in 10 ml of 0.1M KCl solution at pH 2.1. The pH of the resulting 0.5 mM solution of compound **1** was observed to be 2.3 by using pH meter (Eutech instruments). All HER experiments were performed by the help of a Zahner Zanium electrochemical workstation. Electrode potentials were converted to NHE scale using the relation E(NHE) = E(Ag/AgCl) + 0.197V where Ag/AgCl (3M) electrode was used as standard electrode.

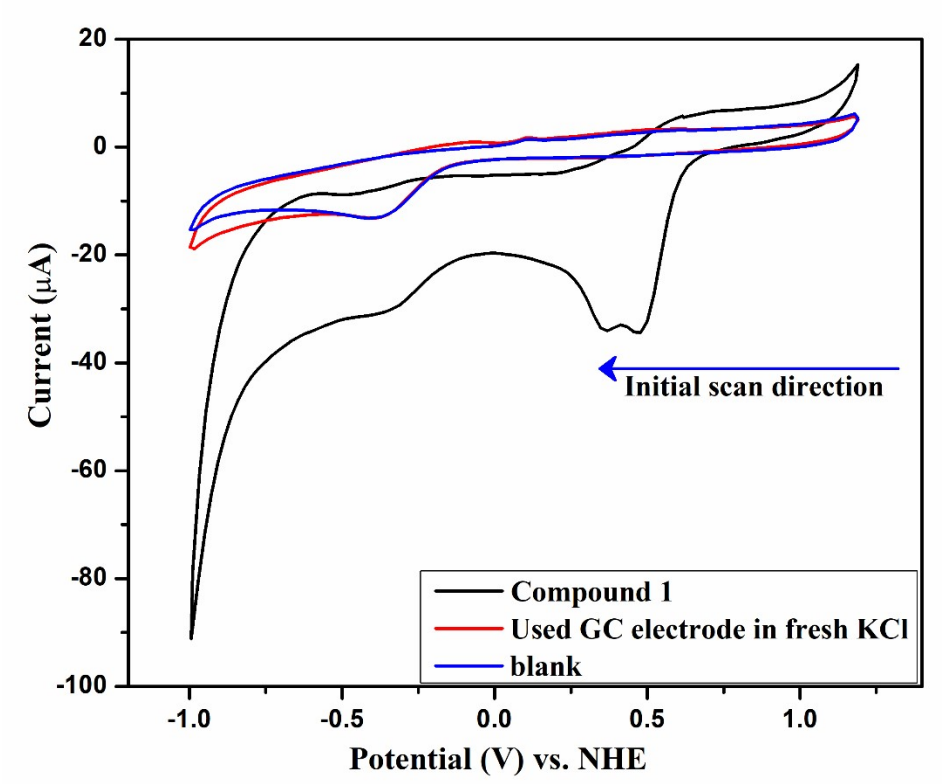

Fig. S8. Controlled experiments to prove that there is no deposition at glassy carbon electrode as working electrode, graphite rod as counter electrode and Ag/AgCl as reference electrode. Blue line is the CV of blank GC electrode in 0.1M KCl at pH 2.3, black line is the CV of 0.5 mM compound **1** in 0.1M KCl at pH 2.3 and red line is the CV of GC electrode after 100 CV cycles in fresh 0.1M KCl at pH 2.3.

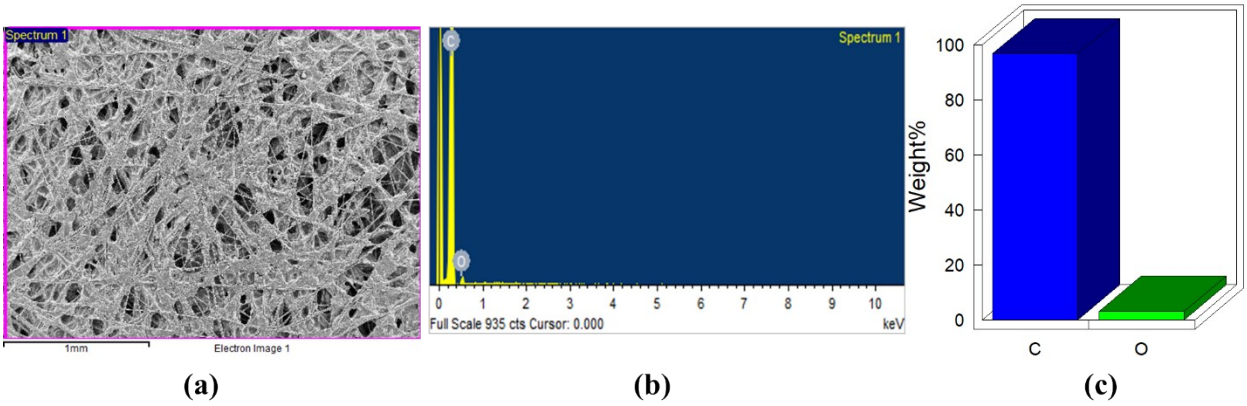

Fig. S9. (a) FESEM image of carbon paper as working electrode after multiple CV cycle (100 Cycles) using graphite rod as counter electrode and Ag/AgCl as reference electrode. (b) Histogram plot for the selected area of the carbon paper. (c) Quantitative analysis of the selected area of the carbon paper.

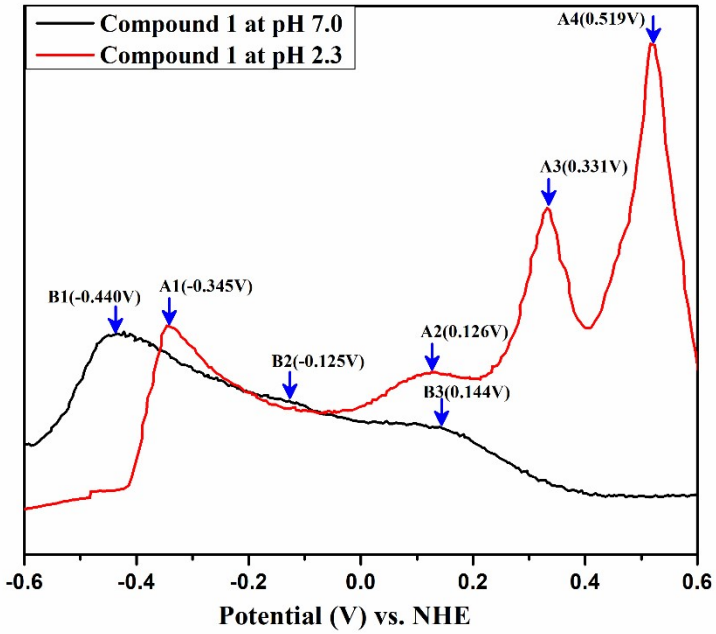

Fig. S10. Differential pulse voltammograms (DPVs) of 0.5 mM compound **1** at pH 2.3 (red line) and 0.5 mM compound **1** at pH 7.0 (black line) in 0.1M KCl.

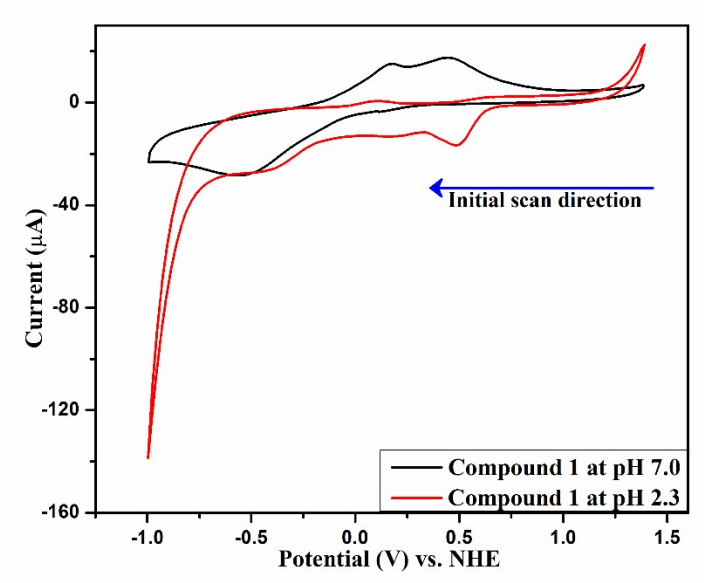

Fig. S11. Cyclic voltammograms (CVs) of 0.5 mM compound **1** at pH 2.3 (red line) and 0.5 mM compound **1** at pH 7.0 (black line) in 0.1M KCl. All the CVs were recorded at the scan rate of 100 mV/s.

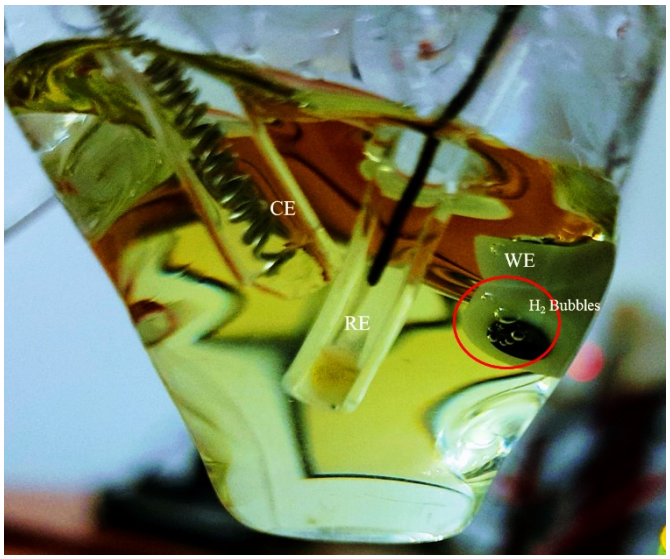

Fig. S12. Image of electrochemical cell consisting glassy carbon electrode as the working electrode (WE), Ag/AgCl electrode as reference (RE) and Pt wire as counter electrode (CE). The bubbles (red circle) at the surface of the glassy carbon electrode during constant potential electrolysis (CPE).

UNIVERSITY OF HYDERABAD--School of chemistry.

Sample Information

Acquired by	: Admin
Sample Name	: Ni-V bulk-2
Sample ID	: Ni-V bulk-2
Tray#	:
Vial#	: 1
Injection Volume	: 0.2
Data File	: Ni-V bulk-2.GCD
Method File	: GC_TCD_gas-SPLIT20.qgm
Batch File	:
Report Format File	:
Date Acquired	: 23-05-2021 09:30:28
Date Processed	: 23-05-2021 09:40:30

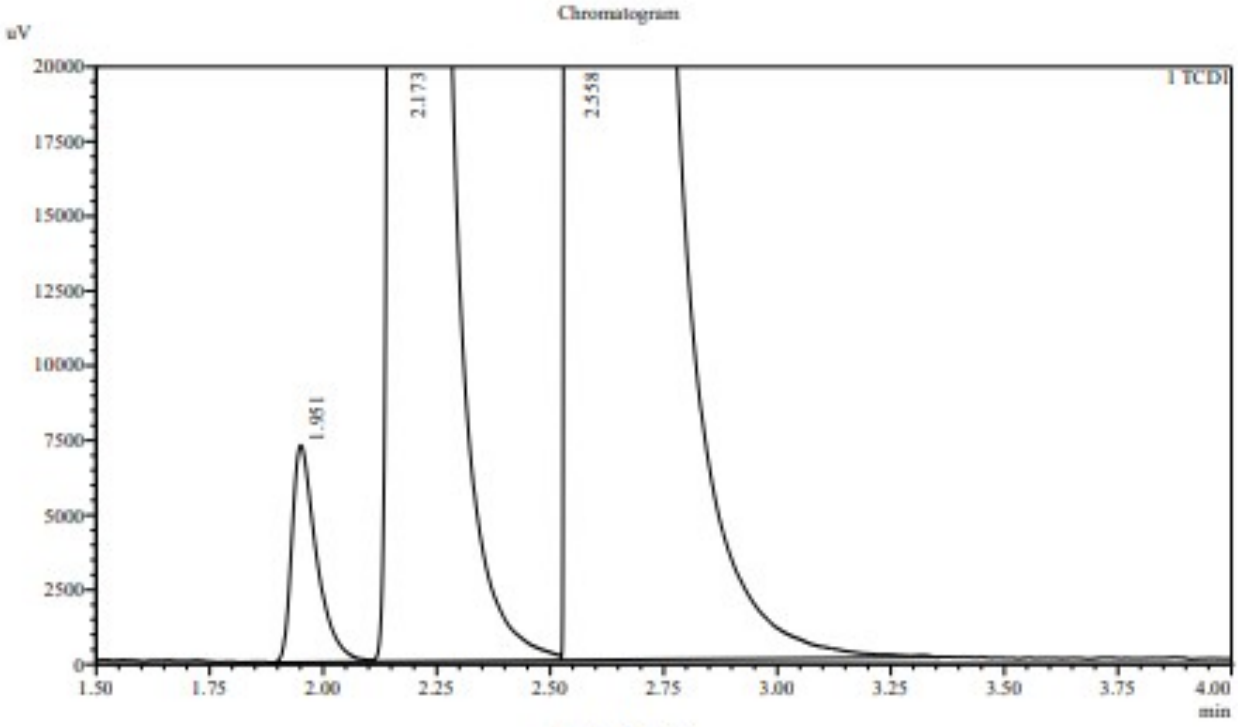

Peak Table

TCD1

Peak#	Ret. Time	Area	Height	Area%	Name
1	1.951	27556	7209	0.580	Hydrogen
2	2.173	1118234	247022	23.542	Oxygen
3	2.558	3604089	551546	75.877	Nitrogen
Total		4749879	805777	100.000	

Fig. S13. Gas chromatography of evolved H_2 gas during bulk electrolysis.

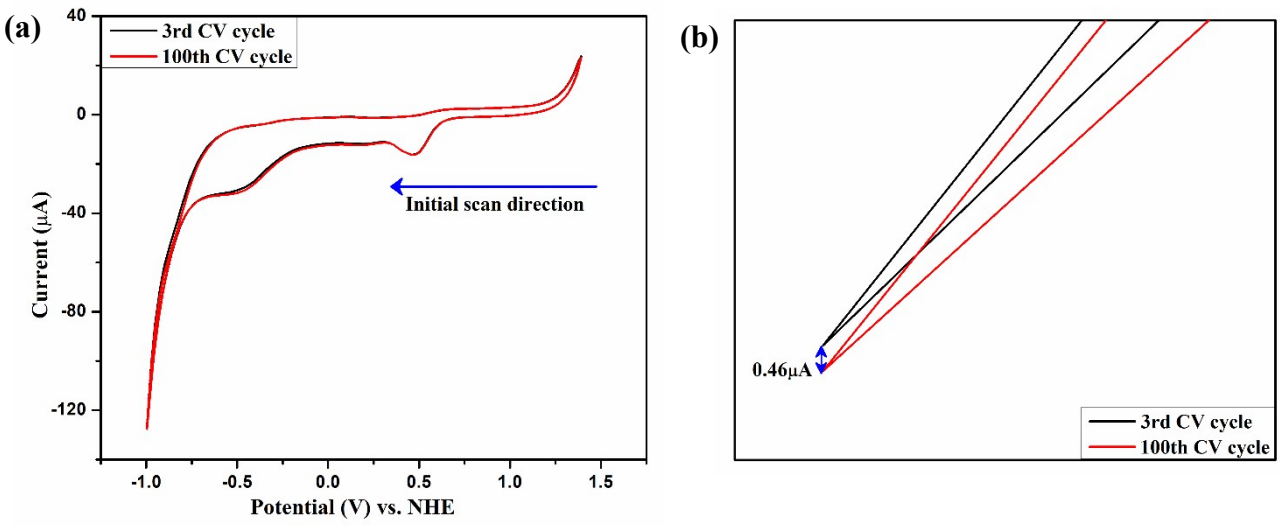

Fig. S14. (a) Stability check of 0.5 mM compound **1** in 0.1M KCl solution at pH 2.3 by 100 CV cycles at a scan rate of 100 mV/s. Black line and red line correspond to 3rd and 100th CV cycles, respectively. (b) Difference between catalytic current of 3rd and 100th CV cycles (0.46 μA).

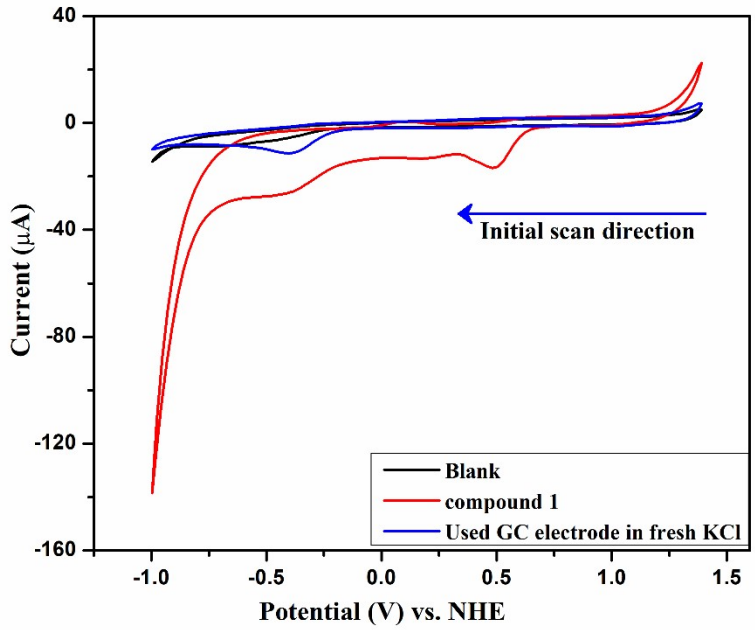

Fig. S15. Controlled experiments to prove that there is no deposition at glassy carbon electrode as working electrode, Pt wire as counter electrode and Ag/AgCl as reference electrode. Black line is the CV of blank GC electrode in 0.1M KCl at pH 2.3, red line is the CV of 0.5 mM compound **1** in 0.1M KCl at pH 2.3 and blue line is the CV of GC electrode after 100 CV cycles in fresh 0.1M KCl at pH 2.3.

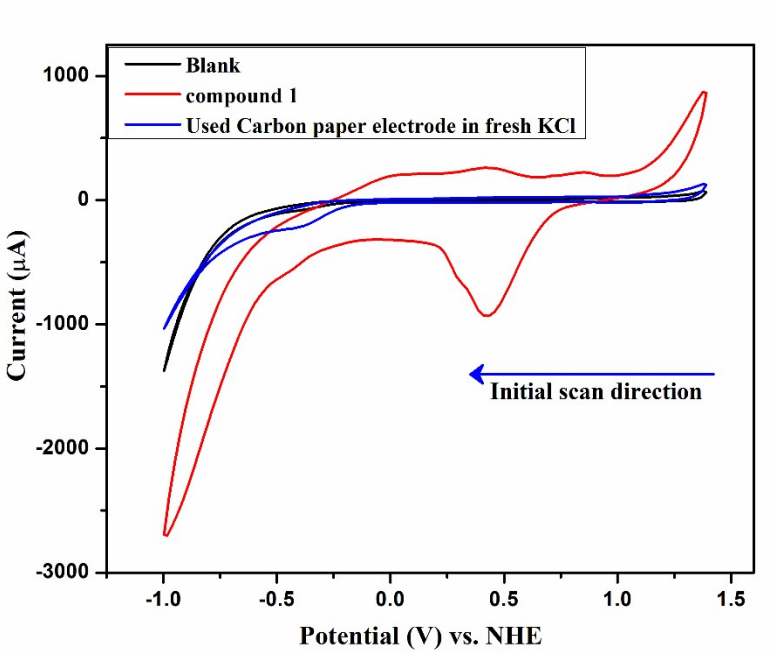

Fig. S16. Controlled experiments to prove that there is no deposition at carbon paper as working electrode, Pt wire as counter electrode and Ag/AgCl as reference electrode. Black line is the CV of blank carbon paper electrode in 0.1M KCl at pH 2.3, red line is the CV of 0.5 mM compound **1** in 0.1M KCl at pH 2.3 and blue line is the CV of carbon paper electrode after 100 CV cycles in fresh 0.1M KCl at pH 2.3.

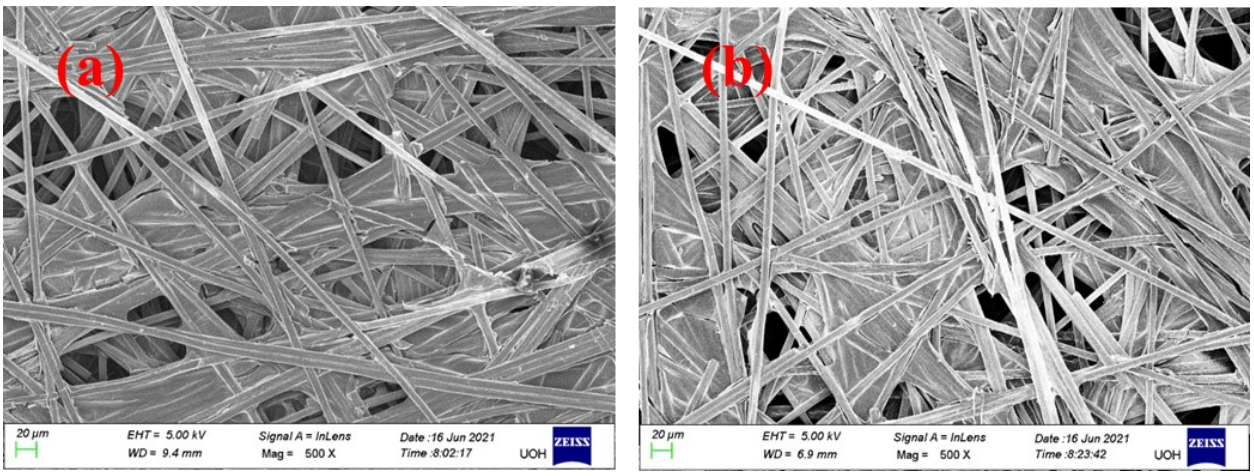

Fig. S17. (a) FESEM image of blank carbon paper and (b) FESEM image of carbon paper after 100 CV cycles.

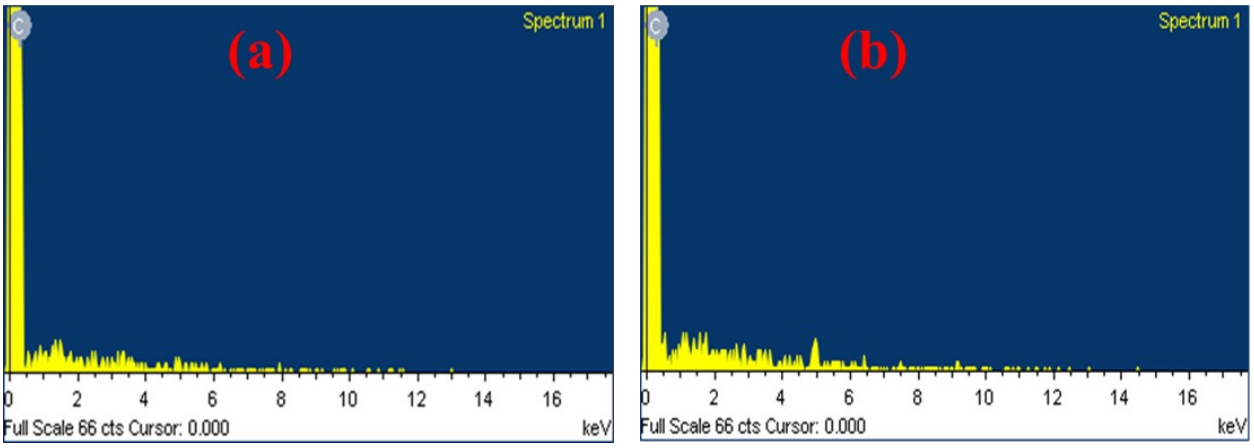

Fig. S18. (a) EDX histogram of blank carbon paper and (b) EDX histogram of carbon paper after 100 CV cycles.

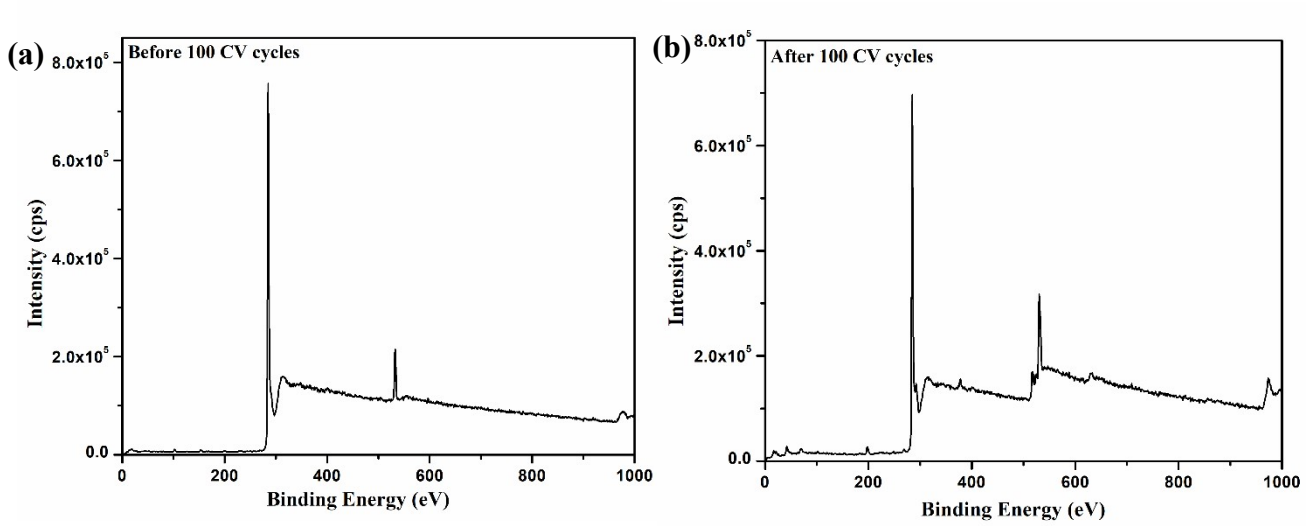

Fig, S19. (a) XPS of blank carbon paper and (b) XPS of carbon paper after 100 CV cycles.

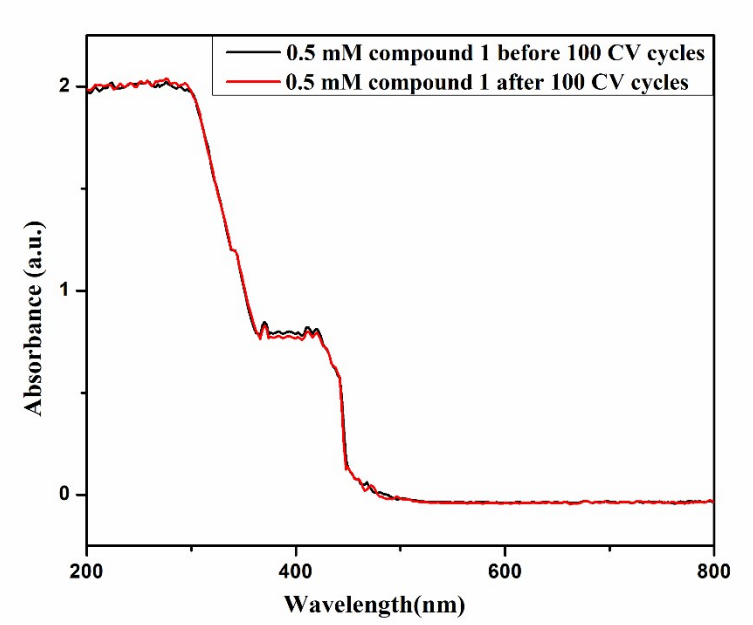

Fig. S20. (a) Stability check of 0.5 mM compound **1** in 0.1M KCl solution at pH 2.3 by UV – visible spectra of 0.5 mM compound **1** before and after 100 CV cycles. Black line and red line correspond to UV-visible spectra of 0.5 mM compound **1** before and after the 100 CV cycles respectively.

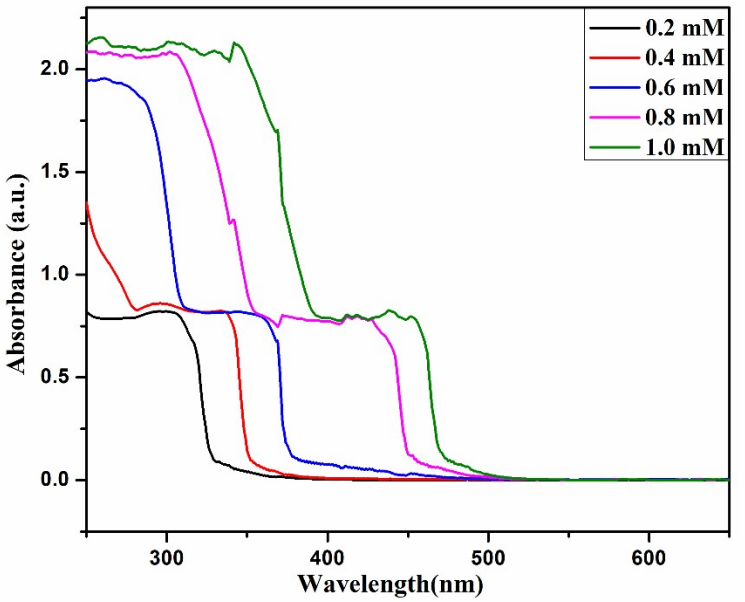

Fig. S21. UV-visible spectra of compound **1** in 0.1M KCl (pH 2.3) at different concentrations (0.2, 0.4, 0.6, 0.8 and 1.0 mM).

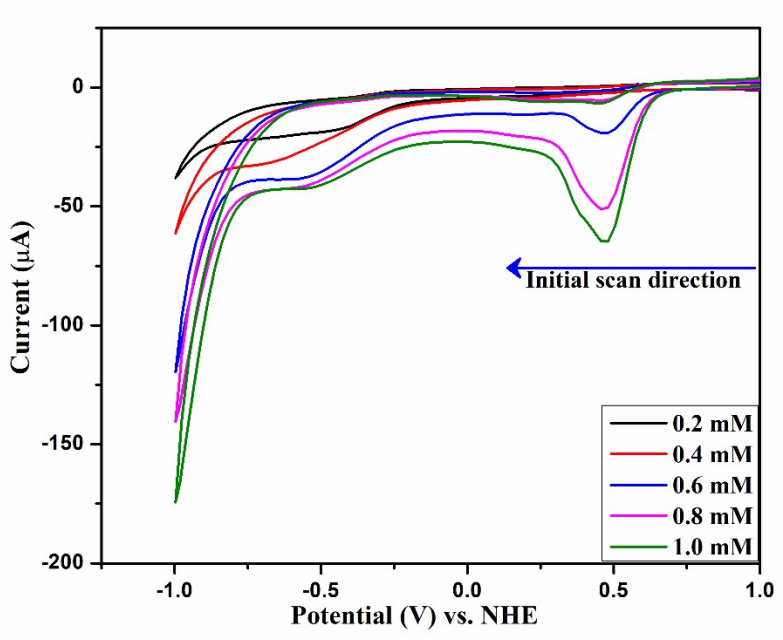

Fig. S22. CV cycles of compound **1** in 0.1M KCl (pH 2.3) at different concentrations (0.2, 0.4, 0.6, 0.8, 1.0 mM).

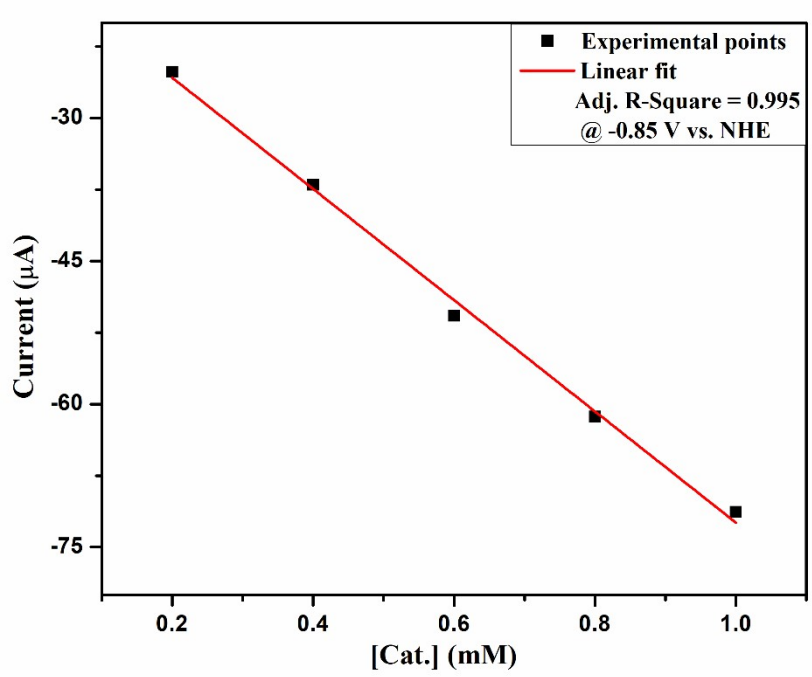

Fig. S23. Plot of catalytic current (i_{cat}) *vs* concentration (from Fig. S22 at the potential of -0.85V vs NHE).

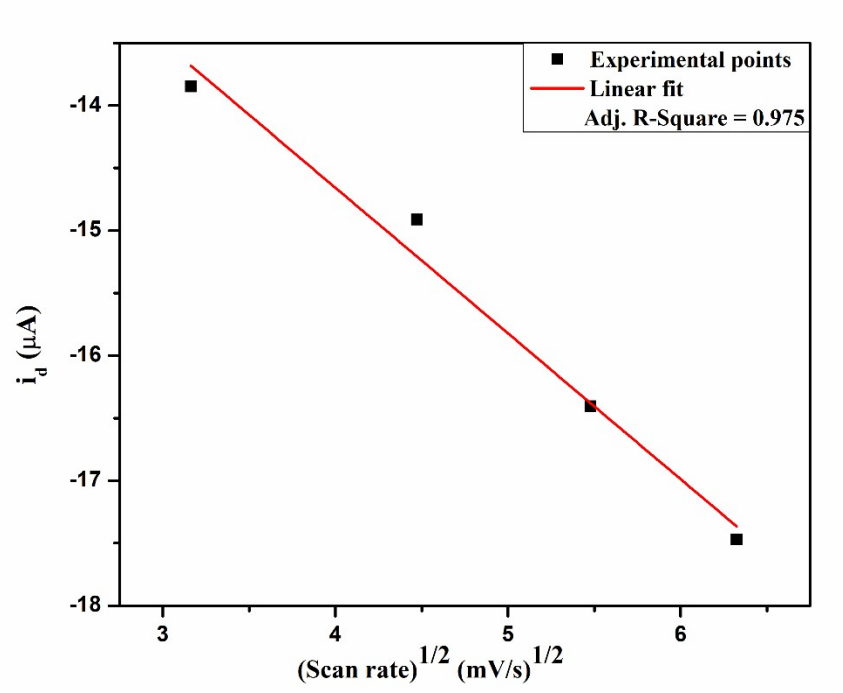

Fig. S24. Plot of peak current (i_d) *vs* square root of scan rate (from Fig. 3b at the potential of -0.45V vs NHE)

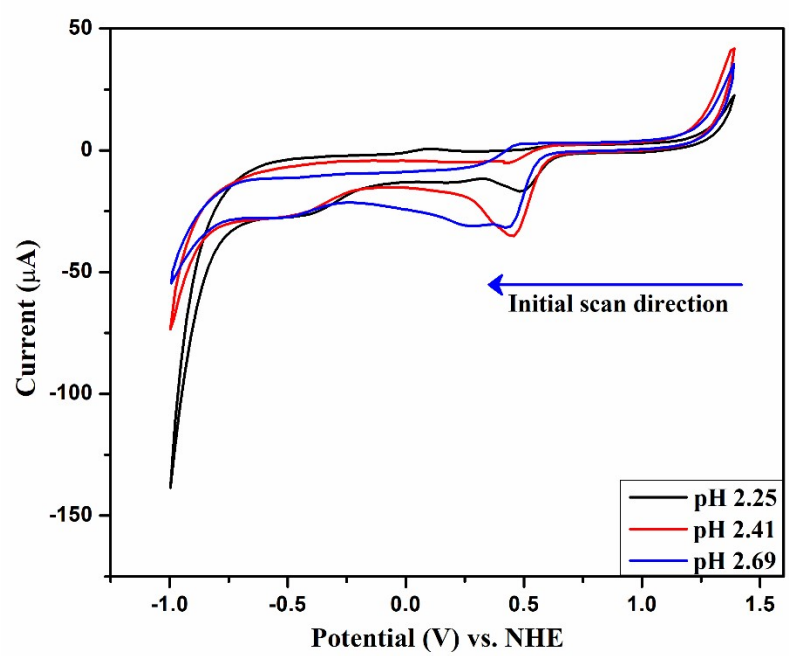

Fig. S25. CV cycles of 0.5 mM compound **1** in 0.1M KCl at different pH values (2.25, 2.41, and 2.69).

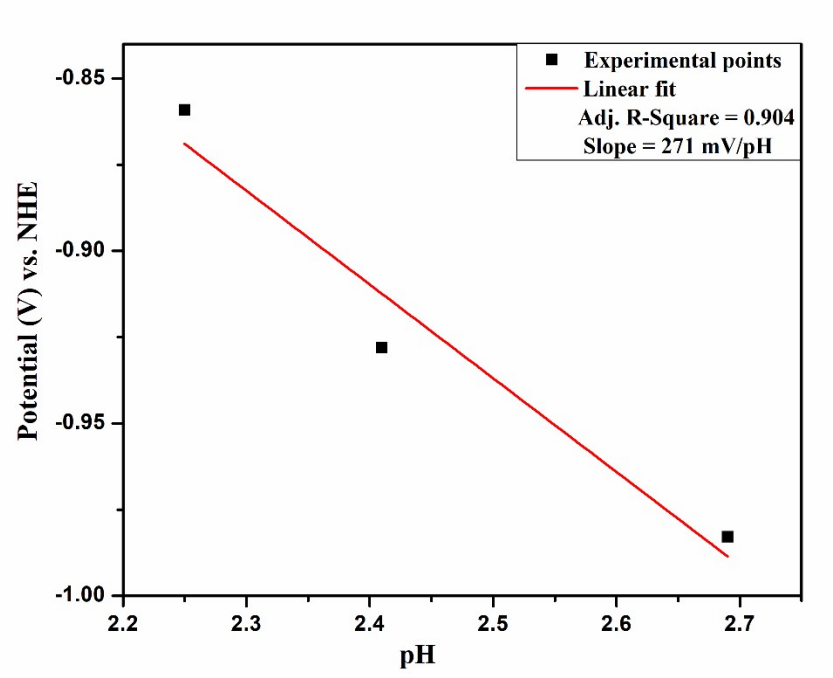

Fig. S26. Plot of potential *vs* pH (from Fig. S25 at the potential of -0.99V vs NHE).

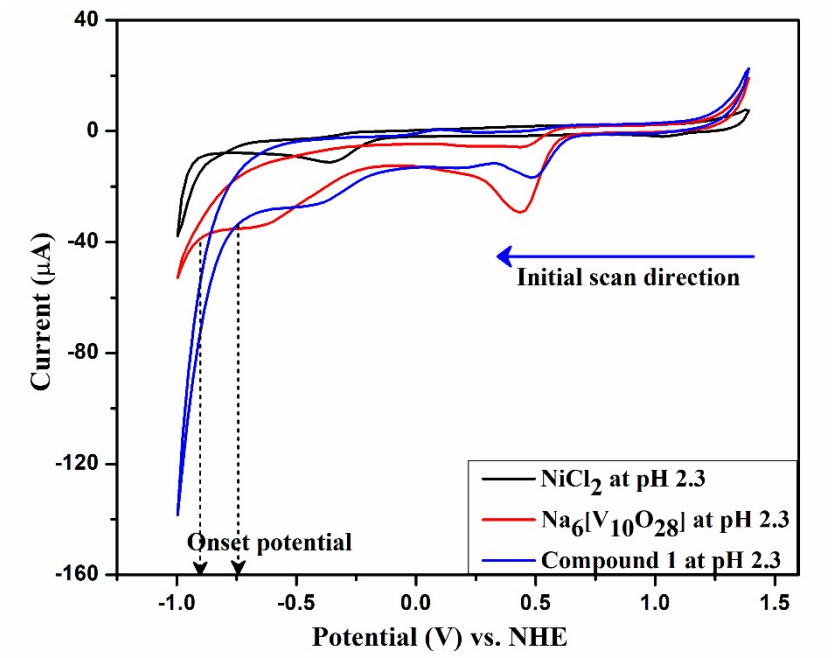

Fig. S27. CVs of 0.5 mM of compound **1** (blue line), $Na_6V_{10}O_{28}\cdot 18H_2O$ (red line), $NiCl_2\cdot 6H_2O$ (black line) at GC electrode in 0.1M KCl at pH 2.3.

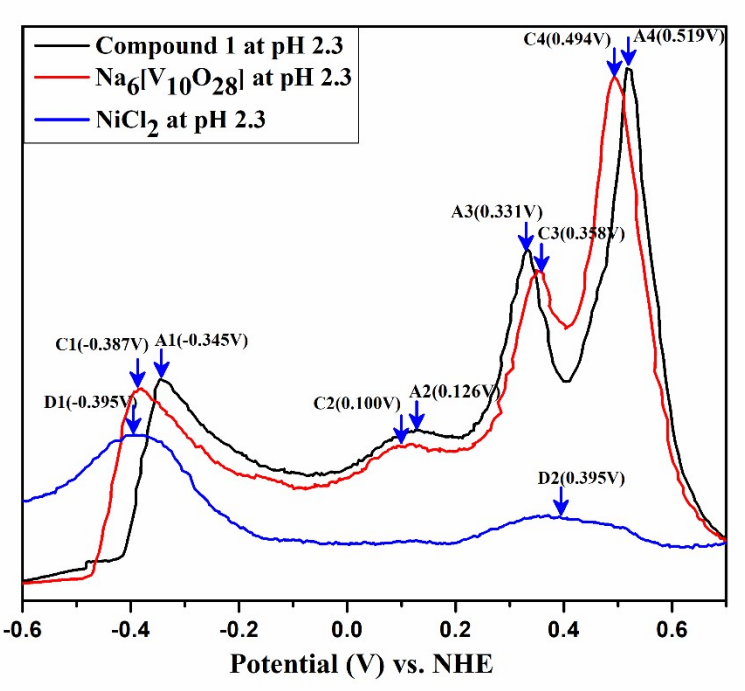

Fig. S28. Differential pulse voltammograms (DPVs) of 0.5 mM compound **1** (black line), 0.5 mM $Na_6[V_{10}O_{28}].18H_2O$ (red line) and 0.5 mM of $NiCl_2$ in 0.1M KCl at pH 2.3 (blue line).

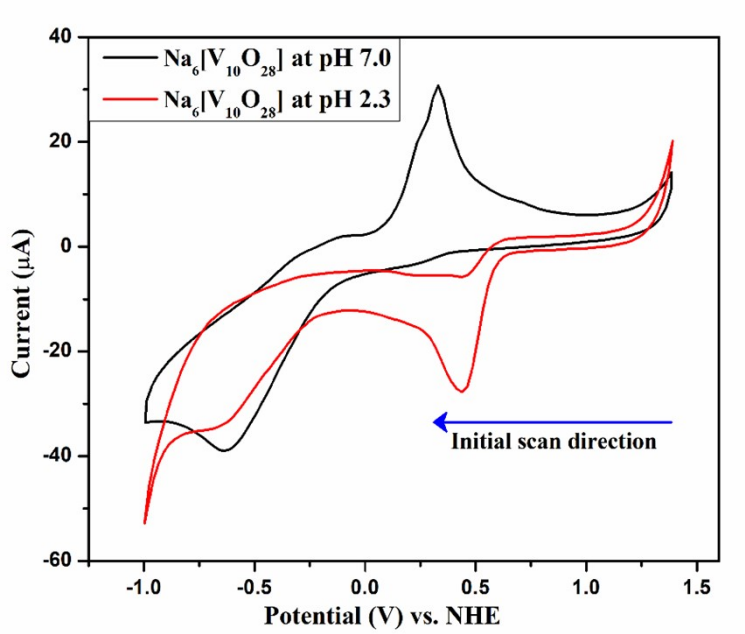

Fig. S29. Cyclic voltammograms (CVs) of 0.5 mM $Na_6[V_{10}O_{28}].18H_2O$ at pH 2.3 (red line) and 0.5 mM $Na_6[V_{10}O_{28}].18H_2O$ at pH 7.0 (black line) in 0.1M KCl. All the CVs were recorded at the scan rate of 100 mV/s.

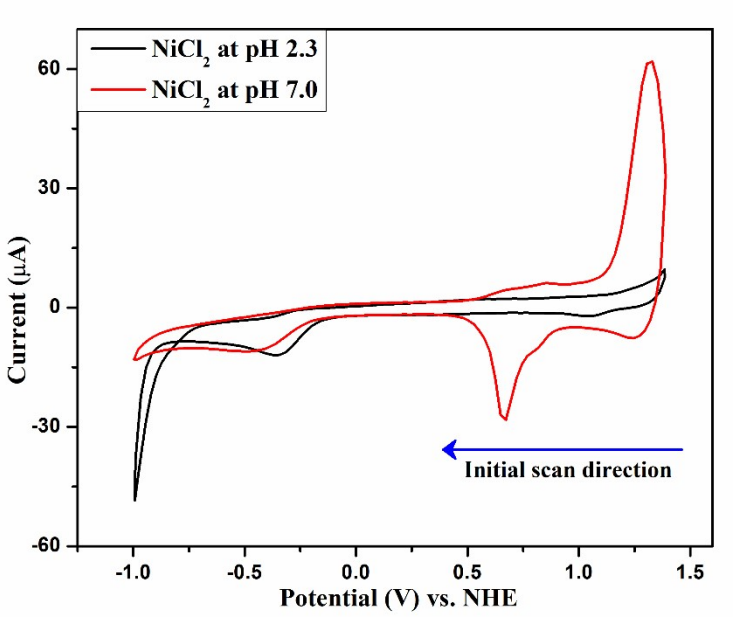

Fig. S30. Cyclic voltammograms (CVs) of 0.5 mM $NiCl_2$ at pH 2.3 (black line) and 0.5 mM $NiCl_2$ at pH 7.0 (red line) in 0.1M KCl. All the CVs were recorded at the scan rate of 100 mV/s.

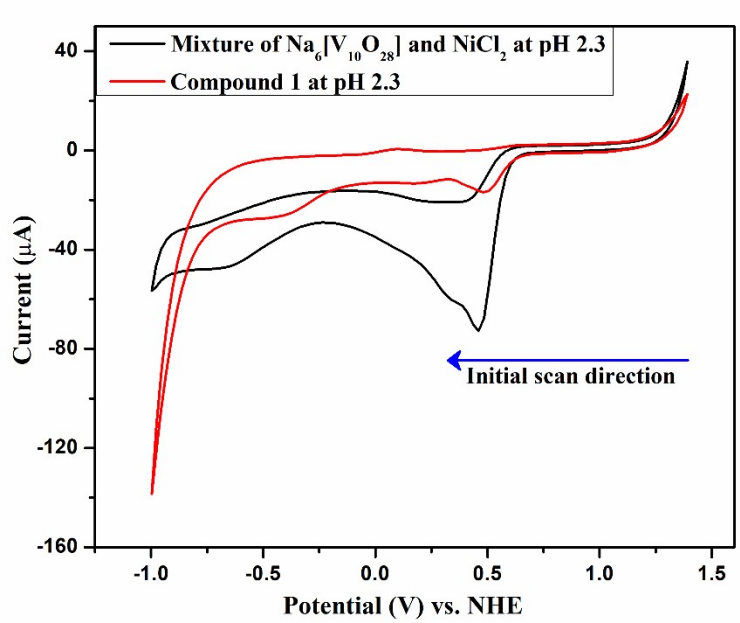

Fig. S31. Cyclic voltammograms (CVs) of 0.5 mM compound **1** at pH 2.3 in 0.1M KCl (red line) and 0.5 mM physical mixture of $Na_6[V_{10}O_{28}].18H_2O$ and $NiCl_2$ (2:1 ratio) at pH 2.3 in 0.1M KCl (black line). All the CVs were recorded at the scan rate of 100 mV/s.

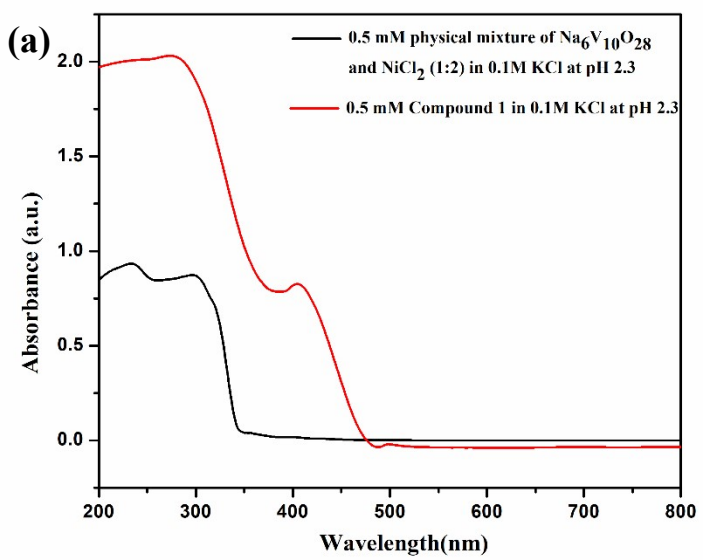

Fig. S32. UV –visible spectra of 0.5 mM compound **1** in 0.1M KCl at pH 2.3 (red) and 0.5 mM of physical mixture of $Na_6[V_{10}O_{28}].18H_2O$ and $NiCl_2$ (1:2) in 0.1M KCl at pH 2.3 (black).

Section S11. Quantitative hydrogen evolution experiment.[7]

Bulk electrolysis was carried out for compound **1** at a constant current density of 1 mA/cm^2 for a period of 5 h with the help of three electrode system in a home-built electrolysis setup. Glassy carbon (GC) electrode of surface area 0.07 cm^2 (diameter 3 mm) was used as working electrode, platinum wire was used as counter electrode and Ag/AgCl electrode as reference electrode. The hydrogen bubbles evolved at the GC electrode during the electrolysis of 0.5 mM of compound **1** in 0.1M KCl at pH 2.3 were gradually collected in a graduated tube of home-built electrolysis setup and slowly it has been displaced with these hydrogen gas bubbles. The oxygen gas which was evolved at the counter electrode could not mix up with the hydrogen gas evolved at working electrode because the setup was built in such a way that gas evolved in the cathodic chamber could not enter into the anodic chamber. The two chambers were separated from each other by an inverted glass tube and a small window has been kept open between them to maintain the electrical continuity.

Fig. S33. Complete set-up of quantitative measurement of evolved H_2 gas by bulk electrolysis in three-electrode system consisting glassy carbon as working electrode, Ag/AgCl (3M) as reference electrode and platinum wire as counter electrode at current density of 1 mA/cm^2.

Calculation of Faradaic efficiency of compound 1:

The amount of hydrogen evolved from the above quantitative measurement in bulk electrolysis at constant current for a time period of 5 h under 1 atm pressure is 0.024 mL/hour.

Thus, the moles of hydrogen evolved in 1 hour = (0.024/22400) mol = **1.0714×10^{-6} mol.**

Whereas the ideal number of moles the hydrogen gas to be evolved is

$$H_2 \text{ (ideal)} = \frac{\text{Q (total charge employed)}}{\text{n (no. of electrons required for the chemical change) x 1 Farad}}$$

where n is 2 for hydrogen evolution reaction as it is a two-electron process and we have employed current of 70 μA.

Here, H_2 (ideal) for 1 h = (70 x 10^{-6} x 3600)/(2 x 96500) mol = **1.3057 x 10^{-6} mol**.

Therefore, the formula for Faradaic efficiency is

$$\text{Faradaic Efficiency} = \frac{\text{Moles of Hydrogen Evolved by experiment}}{\text{Moles of Hydrogen Evolved by ideal}} \times 100$$

Finally, Faradaic efficiency of compound **1** = [(1.0714 x 10^{-6})/(1.3057 x 10^{-6})] x 100 = **82.06%**

Section S12. Determination of overpotential for compound 1:

To determine the overpotential of compound **1**, linear sweep voltammetry (LSV) experiment was performed using three electrode system employing glassy carbon (GC) electrode (3 mm diameter) as working electrode, Pt wire as counter electrode and Ag/AgCl (3M KCl) electrode as reference electrode. This LSV was recorded at the sweep rate of 100 mV/s at room temperature. The electrolyte was 0.5 mM of compound **1** in 0.1M KCl solution at pH 2.3. The electrode potential was converted to NHE scale using the relation E(NHE) = E(Ag/AgCl) + 0.197 V.

Calculation for thermodynamic potential for proton reduction:[2]

When we perform catalytic studies in aqueous medium, Nernst equation (eq 2) was used to calculate the equilibrium potential ($E_{2H^+/H2}$) for proton reduction at 25^0C and 1 atmosphere H_2 from the following equation (eq 2).

$$2H^+ + 2e^- \rightleftharpoons H_2 \qquad (1)$$

$$E_{2H^+/H2} = E^0_{2H^+/H2} - 0.059\text{pH (in V)} \qquad (2)$$

The equilibrium potential for proton reduction ($E^0_{2H^+/H2}$) is 0V vs. SHE (standard hydrogen electrode) at standard condition (pH = 0). This potential is -0.197V vs NHE (normal hydrogen electrode). At pH 2.3 the equation 2 simplifies to equation 3.

$$E_{2H^+/H2} = -0.197 - 0.059 \times 2.3 \text{ (in V)} \qquad (3)$$

= **- 0.3327 V vs. NHE**

Experimentally determining equilibrium potential for proton reduction:

From LSV plot (Figure 3a), we have calculated the $E_{cat/2}$ value which corresponds to experimentally determining equilibrium potential for proton reduction. For compound **1**, the value of $E_{cat/2}$ is **-0.46V vs. NHE.**

Now, the overpotential = $E_{2H^+/H2}$ - $E_{cat/2}$

= -0.3327 - (- 0.46) V

= **127 mV**

Table S3: Important examples of nickel-containing molecular catalyst and compound **1**

Compound	Medium	Overpotential ($E_{cat/2}$) for HER	TOF/TON	Faradaic efficiency	Ref.
$[Ni(dcpdt)_2]^{2-}$	Aqueous, pH = 4-6	330 – 400 mV	TON = 20000 over 24h	92 – 100%	3
$Ni(P^{Cy}_2N^{Gly}_2)$	Aqueous pH = 0.1-9.0	150 – 365 mV	TOF = 1 – 33 s^{-1}	-	4
$[Ni(P^{R'}N^{R''})]^{2+}$	Aqueous, pH = 4.5	200 mV	TOF = 0.128 s^{-1}	85%	5
$[Ni(DHMPE)_2]^{2+}$	Aqueous, pH = 1.0	480 mV	TOF = 1850 s^{-1}	92 – 100%	6
$K_2[Ni(OH_2)_6]_2[V_{10}O_{28}].4H_2O$	Aqueous, pH = 2.3	127 mV	TOF = 2.1 s^{-1}	82%	This work

Reference:

(1) M. Nadjafi, P. M. Abdala, R. Verel, D. Hosseini, O. V. Safonova, A. Fedorov and C. R. Müller, *ACS Catal.,* 2020, **10**, 2314-232.
(2) A. M. Appel and M. L. Helm, *ACS Catal.,* 2014, **4**, 630-633.
(3) K. Koshiba, K. Yamauchi and K. Sakai, *Angew. Chem. Int. Ed.,* 2017, **56**, 4247 –4251.
(4) A. Dutta, S. Lense, J. Hou, M. H. Engelhard, J. A. S. Roberts and W. J. Shaw, *J. Am. Chem. Soc.,* 2013, **135**, 18490-18496.
(5) M. A. Gross, A. Reynal, J. R. Durrant and E. Reisner, *J. Am. Chem. Soc.,* 2014, **136**, 356-366.

(6) C. Tsay and J. Y. Yang, *J. Am. Chem. Soc.,* 2016, **138**, 14174−14177.
(7) S. Mukhopadhyay, J. Debgupta, C. Singh, A. Kar and S. K. Das, *Angew. Chem.,* 2018, **130**, 1936 –1941.

****